Earthq Eng & Eng Vib (2019) 18: 497-509 **DOI**: https://doi.org/10.1007/s11803-019-0517-6

Site dependent and spatially varying response spectra

Hakima Djilali Berkane[1†], Zamila Harichane[1‡], Erkan Çelebi[2‡] and Sidi Mohammed Elachachi[3‡]

1. *Geomaterials Laboratory, Hassiba Benbouali University of Chlef, Chlef 02180, Algeria*
2. *Department of Civil Engineering, Sakarya University, Adapazari, Turkey*
3. *University of Bordeaux, I2M, GCE Department, France*

Abstract: The goal of this study is to provide a stochastic method to investigate the effects of the randomness of soil properties due to their natural spatial variability on the response spectra spatial variation at sites with varying conditions. For this purpose, Monte Carlo Simulations are used to include the variability of both incident ground motion and soil parameters in the response spectra by mean of an appropriate coherency loss function and a site-dependent transfer function, respectively. The approach is built on the assumption of vertical propagation of SH type waves in soil strata with uncertain parameters. The response spectra are obtained by numerical integration of the governing equation of a single-degree-of-freedom (SDOF) system under non-stationary site-dependent and spatially varying ground motion accelerations simulated with non-uniform spectral densities and coherency loss functions. Numerical examples showed that randomness of soil properties significantly affects the amplitudes of the response spectra, indicating that as the heterogeneity induced by the randomness of the parameters of the medium increases, the spectral ordinates attenuate.

Keywords: response spectra; randomness; spectral density; Monte Carlo

1 Introduction

Previous studies highlighted the significant effects of the ground motion spatial variation on the seismic response of long structures (Zerva, 1992; Saxena *et al*., 2000; Lin *et al*., 2004; Chouw and Hao, 2005, 2008). This spatial variation is usually related to the effects of local soil conditions, wave passage and incoherency (Mwafy *et al*., 2011). The first one expresses the effect of local soil conditions at a site (Hao *et al*., 1989). The second one translates the phase difference in seismic waves at various structure support points, while the third source is attributed to the scattering in the heterogeneous ground. Various methods were extensively used by several researchers to study the response of long structures excited by motions varying in space and time (Hao, 1998; Yang *et al*., 2002; Lou and Zerva, 2005; Konakli and Der Kiureghian, 2011; Davoodi *et al*., 2013; Zhang *et al*., 2013, 2014; Alam and Kim, 2014, Adanur *et al*., 2016).

The response spectrum method satisfactorily describes the seismic ground motion features (Djilali Berkane *et al*., 2014, 2018) and is still an attractive methods for the engineering community over the past few decades.

On other hand, analyses and design of relevant structures require in many cases the use of both recorded and artificial time-histories ground motion. However, it is not often possible to sufficiently record seismic motions in a specified site, particularly in areas with low seismicity levels. Thus, artificial simulation of ground motions is inevitable for structural design. Nevertheless, the occurrence of an earthquake generates waves which propagate in several directions, the most important of which for this type of study is towards the ground surface of a given site. However, this wave path may be altered by soil conditions and source patterns. An adequate accounting of the subsequent actions and rigorous modelling of the ground motion may be only afforded in a probabilistic framework, especially since the earthquake itself is of a random nature (Cacciola and D'Amico, 2015; He, 2015).

Since the SMART-1 array installation, the spatial variation of seismic ground motions has been modelled by many researchers and several models have been proposed (Zerva and Zervas, 2002). Two functions are commonly used to model the spatial variation of seismic ground motions: spectral density and loss of coherence. (Harichandran and Vanmarke, 1986; Loh and Lin, 1990; Der Kiureghian, 1996). Cacciola and Deodatis (2011)

Correspondence to: Zamila Harichane, Geomaterials Laboratory, Hassiba Benbouali University of Chlef, P.O. Box 151, Chlef 02180, Algeria
Tel: +213 (0) 27729398; Fax: +213 (0) 27727055
E-mail: z_harichane@yahoo.fr
†PhD; ‡Professor

Received December 19, 2017; **Accepted** May 7, 2018

have offered a methodology using spectral-representation to generate multiple surface non-stationary and spectrum-compatible ground motions taking advantage of the Monte Carlo powerful methods. Bi and Hao (2012) have suggested a procedure for modelling and simulation of time-history accelerations at several locations on irregular ground surfaces using a deterministic 1-D wave propagation theory and incoherence function to derive the surface motions spectral densities at an uneven site. Li *et al*. (2018) presented an approach to model and simulate the multi-support depth-varying seismic motions within heterogeneous offshore and onshore sites based on 1D wave propagation theory and considering the effects of seawater and porous soils on the propagation of seismic P waves. Yazdani and Takada (2011) used simulated (or artificial) time-histories instead of recorded accelerograms to calculate the response spectrum based on Fourier Amplitude Spectra (FAS), which showed that uncertainties that may affect response spectra are mainly due to the variability of the soil conditions.

The natural spatial variability of soil properties may be a source of uncertainty (Phoon and Kulhawy, 1999; Elkateb *et al*., 2002; Popescu *et al*., 2005). This kind of uncertainty, also referred to as inherent random variability, may strongly alter the behavior of loaded soils (Popescu, 2008). Several researchers studied the influence of the uncertainties of soil properties on the earthquake response of soil deposits (Gao *et al*., 2008; Hacıefendioğlu, 2010; Badaoui *et al*., 2010; Li and Assimaki, 2010; Bi and Hao, 2011; Sadouki *et al*., 2012; Sadouki *et al*., 2018).

In this paper, a methodology for simulation of site-dependent and spatially varying response spectra is proposed. The incident motion is assumed to have the same base rock spectral density at selected locations and is modelled by the Clough and Penzien (1993) filter and its spatial variation is described by a coherency function. The vertical dependence of ground motions on the soil conditions through multiple layers of soil profiles is obtained under the assumption of one dimensional propagation of SH-type waves (Wolf, 1985). The contribution of the soil layers brought by the inherent randomness of the variability of the soil properties in the spatial variation of seismic response spectra is considered by means of the amplification function and power spectral density function (PSD) by assuming the characteristics of the soil profiles as random variables. Gaussian variables of these parameters are sampled many times using the Monte Carlo method. The obtained site dependent amplification functions and power spectral density functions are used to generate ground accelerations varying in space. Then, ground surface response spectra are obtained by numerically solving the governing equation of a single-degree-of-freedom oscillator subjected to the generated non-stationary accelerations.

2 Simulation of spatially varying ground motions

The base rock incident motion is commonly supposed as a stationary random process having the same spectral density (PSD) function at different locations (Fig. 1) and is modelled by the filter of the Clough and Penzien (1993) PSD function

$$S_{\mathrm{g}}(\omega)=\frac{\omega^4}{\left(\omega_{\mathrm{f}}^2-\omega^2\right)^2+\left(2\xi_{\mathrm{f}}\omega_{\mathrm{f}}\omega\right)^2}\cdot \frac{\omega_{\mathrm{g}}^4+\left(2\xi_{\mathrm{g}}\omega_{\mathrm{g}}\omega\right)^2}{\left(\omega_{\mathrm{g}}^2-\omega^2\right)^2+\left(2\xi_{\mathrm{g}}\omega_{\mathrm{g}}\omega\right)^2}\cdot S_0 \tag{1}$$

where S_0 is the white noise base rock excitation spectral density. ω_{g} and ξ_{g} are the natural frequency and damping, respectively, of the soil deposit modelled by the Clough and Penzien (1993) filter and ω_{f} and ξ_{f} are those of the second filter (in Eq. (1)). This assumption is realistic when the site is sufficiently distant from the earthquake focus than to the others sites.

The cross PSD matrix at (n) bedrock locations can be derived as (Hao *et al*., 1989):

$$S_{j'k'}(\mathrm{i}\omega)=S_g(\omega)\gamma_{j'k'}\left(d_{j'k'},\mathrm{i}\omega\right);\ j',k'=1,\ n;\ j'\neq k' \tag{2}$$

where $\gamma_{j'k'}\left(d_{j'k'},\mathrm{i}\omega\right)$ is the base rock incoherency, i the complex number ($\mathrm{i}^2=-1$), w the excitation frequency and $d_{j'k'}$ is the separation distance between two base rock positions, j' and k'.

The cross-PSD matrix of the ground surface motions, considering the effects of local soil conditions, is given by Eq. (3), stating the cross-PSD functions between the spatial (n) bedrock points (j', k') and corresponding (n) ground surface (j, k) points as

$$\boldsymbol{S}_{jk}(i\omega)=H_j(i\omega)H_k^*(i\omega)S_{j'k'}(i\omega);\ j,k,j',k'=1,n \tag{3}$$

In Eq. (3), $H_j(\mathrm{i}\omega)$ and $H_k(\mathrm{i}\omega)$ are the amplification functions of profiles j-j' and k-k' (Fig. 1), respectively.

The Cholesky decomposition method may be used to write the cross-PSD matrix $\boldsymbol{S}_{jk}(\mathrm{i}\omega)$ (Eq. (3)) as follows:

$$\boldsymbol{S}_{jk}(\mathrm{i}\omega)=\boldsymbol{L}(\mathrm{i}\omega)\boldsymbol{L}^{\mathrm{H}}(\mathrm{i}\omega) \tag{4}$$

where $\boldsymbol{L}(\mathrm{i}\omega)$ and $\boldsymbol{L}^{\mathrm{H}}(\mathrm{i}\omega)$ are the lower triangular and Hermitian matrix, respectively.

The Fast Fourier transform process may be followed to simulate stationary frequency-histories (Hao *et al*., 1989)

$$Y_j(\mathrm{i}\omega)=\sum_{m=1}^{j}\beta_{jm}(\omega_\mathrm{n})[\cos\alpha_{jm}(\omega_\mathrm{n})+\mathrm{i}\sin\alpha_{jm}(\omega_\mathrm{n})] \quad (5)$$

with

$$\alpha_{jm}(\omega_\mathrm{n})=\beta_{jm}(\omega_\mathrm{n})+\varphi_{mn}(\omega_\mathrm{n}) \quad (6a)$$

$$\beta_{jm}(\omega)=\tan^{-1}\left(\frac{\mathrm{Im}[L_{jm}(\mathrm{i}\omega)]}{\mathrm{Re}[L_{jm}(\mathrm{i}\omega)]}\right) \quad (6b)$$

$\alpha_{jm}(\omega_\mathrm{n})$ are the amplitudes of the generated motions and $\beta_{jm}(\omega)$ is their phase angles. φ_{mn} is the phase angle randomly created in the interval [0, 2π] according to the uniform distribution function. N_f is the total number of discrete frequencies ($\omega_\mathrm{n}=i_\mathrm{f}\Delta\omega$ where i_f is the frequency number sampling $i_\mathrm{f}=1, N_\mathrm{f}$ and $\Delta\omega=\omega_\mathrm{u}/N_\mathrm{f}$) (Deodatis, 1996; Hao *et al*., 1989). ω_u represents an upper cut-off frequency.

The Inverse Fast Fourier Transform of $Y_j(\mathrm{i}\omega)$ leads to the corresponding time-histories $y_j(t)$.

In this study, multiple locations of non-stationary seismic accelerations result by multiplying $y_j(t)$ by a deterministic modulation function $A(t)$ according to Eq. (7) (Shrikhande and Gupta, 1998):

$$\ddot{u}_j(t)=A(t)y_j(t) \quad (7)$$

$\ddot{u}_j(t)$ is called a zero-mean nonstationary random process of separable kind (Giaralis and Spanos, 2012) and

$$A(t)=\begin{cases}\left(\dfrac{t}{t_0}\right)^2 & 0\le t\le t_0\\ 1 & t_0<t\le t_n\\ \exp\left[-0.155\left(t-t_n\right)\right] & t_n<t\le T\end{cases} \quad (8)$$

Here T is the duration of motion. The quantities t_0 and t_n are any portions of the total duration (Clough and Penzien, 1993).

3 Site dependent ground motions

Under the assumptions of vertical SH wave propagation and horizontally stratified soil deposits, the locations 1, 2 and 3 are expected to be sufficiently distant (Harichane *et al*., 2005). The governing equation in each linear elastic layer l (l = 1, N_C where N_C is the layers number in a soil column *j-j'*) of each nonhomogeneous soil deposit (Fig. 1) is

$$\frac{\partial^2 u_l\left(z_{jl},t\right)}{\partial t^2}=V_{sl}^2\frac{\partial^2 u_l\left(z_l,t\right)}{\partial z^2} \quad (9)$$

where V_{sl} is the velocity in the lth layer. The solution of Eq. (9) may be obtained for a harmonic motion in the form of Eqs. (A1)-(A2) in the appendix.

The amplification (or transfer) function $H(\mathrm{i}\omega)$ for each site is the ratio of the displacement amplitude at the free surface of the soil deposit (l = 1 and z_l = 0 in Eq. (A2) to that at the interface between the soil and the bedrock ($l=N_\mathrm{c}+1$ and $z_{Nc+1}=0$ in):

$$H(\mathrm{i}\omega)=\frac{2A_\mathrm{I}}{A_{Nc+1}+A'_{Nc+1}} \quad (10)$$

where A_I and A_{Nc+1} are the amplitudes of the incident waves at free surface and at bedrock, respectively, and A'_{Nc+1} is that of the reflected wave at bedrock (Eqs. (A3)-(A4)).

4 Methodology for Monte Carlo simulations

Due to the inherent variability of soil properties commonly treated by stochastic or probabilistic methods,

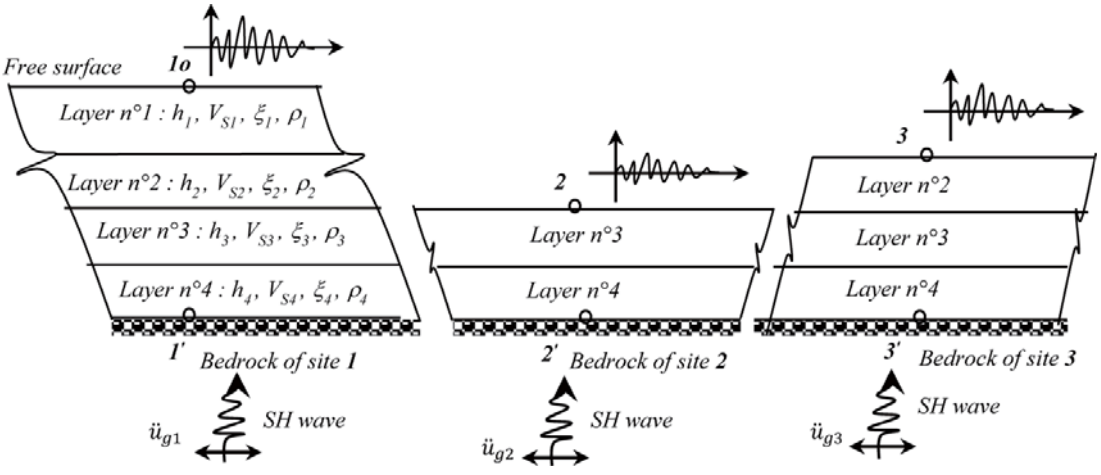

Fig. 1 Schematic view of the soil profiles of the sites

the randomness of soil properties cannot be neglected. Many methods are used to consider the randomness of soil properties. However, the most powerful and practical methods are the Monte Carlo methods (MCMs) (Elkateb *et al*., 2002; Cho, 2007; Popescu, 2008; Guellil *et al*., 2017). Referring to several research papers and textbooks, it is stated that for analysis purposes, the inherent spatial variation of soil properties is usually accounted for by an average value and fluctuations around the average value (coefficient of variation C_v). The relevant parameters that govern the amplification function are the thickness, velocity, damping and mass density of each layer. However the randomness of mass density in terms of C_v up to 20% does not exert a significant effect on the amplification function (Sadouki *et al*., 2012). Thus, the three remaining parameters are treated in the present study as statistically dependent or independent Gaussian variables with mean values and C_v.

With Monte Carlo methods, a deterministic problem may be solved several times by randomly generating several thousand samples of each soil parameter (Sadouki *et al*., 2018; Djilali Berkane *et al*., 2019). For every generated sample of each soil parameter, the amplification function (Eq. (10)) and the PSD (Eq. (3)) are computed according to a predefined probability distribution function. For a satisfactory number of samples of each one of the three variables, the mean transfer function and cross-PSD function amplitudes are obtained. The process is repeated many times in the frequency domain and the generation of spatially varying ground motions is performed. Then, the accelerations time-histories are obtained using the Fast Fourier transform technique. Finally, the ground surface site dependent and spatially varying response spectra are obtained by numerical integration of the governing equation of the SDOF oscillator (Eqs. (A5)–(A7)) in appendix) subjected to non-stationary ground acceleration. This procedure is transcribed numerically as shown in the algorithm in Fig. 2.

5 Results and discussions

5.1 Stochastic amplification functions

The assumption of vertical propagation of shear waves is expected to be satisfied because the waves are refracted to a near-vertical direction due to the decrease in velocities of the surface deposits.

Inhomogeneous soil profiles of sites (Fig. 1) are arbitrary established by varying soil conditions in both the horizontal and vertical directions. The soil profiles under points 1, 2, and 3 are assumed to consist of four layers, two layers and three layers, respectively, overlaying bedrock. The layers are numbered 1(top layer) to N_c+1 (half space) where each l layer is characterized by its thickness h_l, shear wave velocity V_{sl}, damping ratio ξ_l and mass density ρ_l as shown in Table 1.

The mean amplification function is first computed taking into account the randomness of the three above parameters with the help of Monte Carlo methods. Mean

Begin
Initialize data (read mean and standard deviation (or C_v) for parameters
For *is* 1 to *Np* **do** (*Ns : number of sites*)
For *jf* 1 to *Nfr* **do** (*Nfr : number of frequencies*)
$\omega_n = j_f \Delta\omega$ (*$\Delta\omega$ is the frequency step*)
For *ir* = 1 to *Nrand* **do** (*Nrand : number of sampled variables*)
Sampling Gaussian random variables

For *j* = 1 to *Nc(i)* **do** (*Nc(i) : the number of layers*)
Calculate amplitudes of incident and reflected waves (*Eqs. (A3) and (A4) in Appendix)*
for each random number

end for
Calculate mean transfer and cross-PSD functions (*using Eqs. (10) and (3))*
for each frequency
end for
Simulate ground acceleration frequency domain at the (*using Eq. (5))*
different base rock or ground surface locations and
convert them into time domain using the FFT

Then obtain the non-stationary acceleration time histories (*using Eq. (7))*
Finally, obtain the ground surface site dependent and spatially (by solving *Eq. (A5) in appendix)*
varying response spectra, at the different ground surface locations
end for
End (*Program terminated)*

Fig. 2 Algorithm of the stochastic approach for simulating ground motion response

Table 1 Mean values of soil layers parameters

Layer's number	layer's thickness h (m)	Wave velocity V_S (m/s)	Mass density ρ (kg/m^3)	Damping ratio ζ (%)
1	05	150	1900	5
2	10	220	2000	5
3	10	50	2100	5
4	15	500	2200	5
Bedrock	-	884	2300	5

values of the soil parameters are shown in Table 1 for each one of the layers composing the site soil profiles in Fig. 1. The randomness of the soil properties is taken into account by several coefficients of variation C_v (0%, 10%, 15% and 20%), 0% corresponds to the deterministic case.

Figure 3 shows the influence of randomness of the wave velocity, thickness and damping ratio of each layer on the amplification function of each one of the three sites shown in Fig. 1. This figure reveals that when the fluctuation sizes in (C_v) of the velocity and thickness increase, the amplification function amplitudes decrease with an enlargement of the frequency contents (Figs. 3(a)-3(b)). 20% C_v of the wave velocity reduces the amplification function amplitudes of 66.7%, 71.2% and 68.2%, compared to the deterministic solution, for sites 1, 2 and 3, respectively, at the fundamental frequencies (Figs. 3(a), 3(b) and 3(c)). While for 20% C_v of the layer's thickness, the same amplification function amplitudes are reduced by 61.3%, 67.4%, 71.6% for sites 1, 2 and 3, respectively, at the fundamental frequencies with a light shift of the natural frequency to the left for site 1 (Figs. 3(d), 3(e), 3(f)). However, the random variations of the damping ratio do not exert any influence (Figs. 3(g), 3(h), 3(i)). A comparison between the amplification functions of sites 1, 2, 3 shows their sensitivity to the spatial variation of the soil conditions.

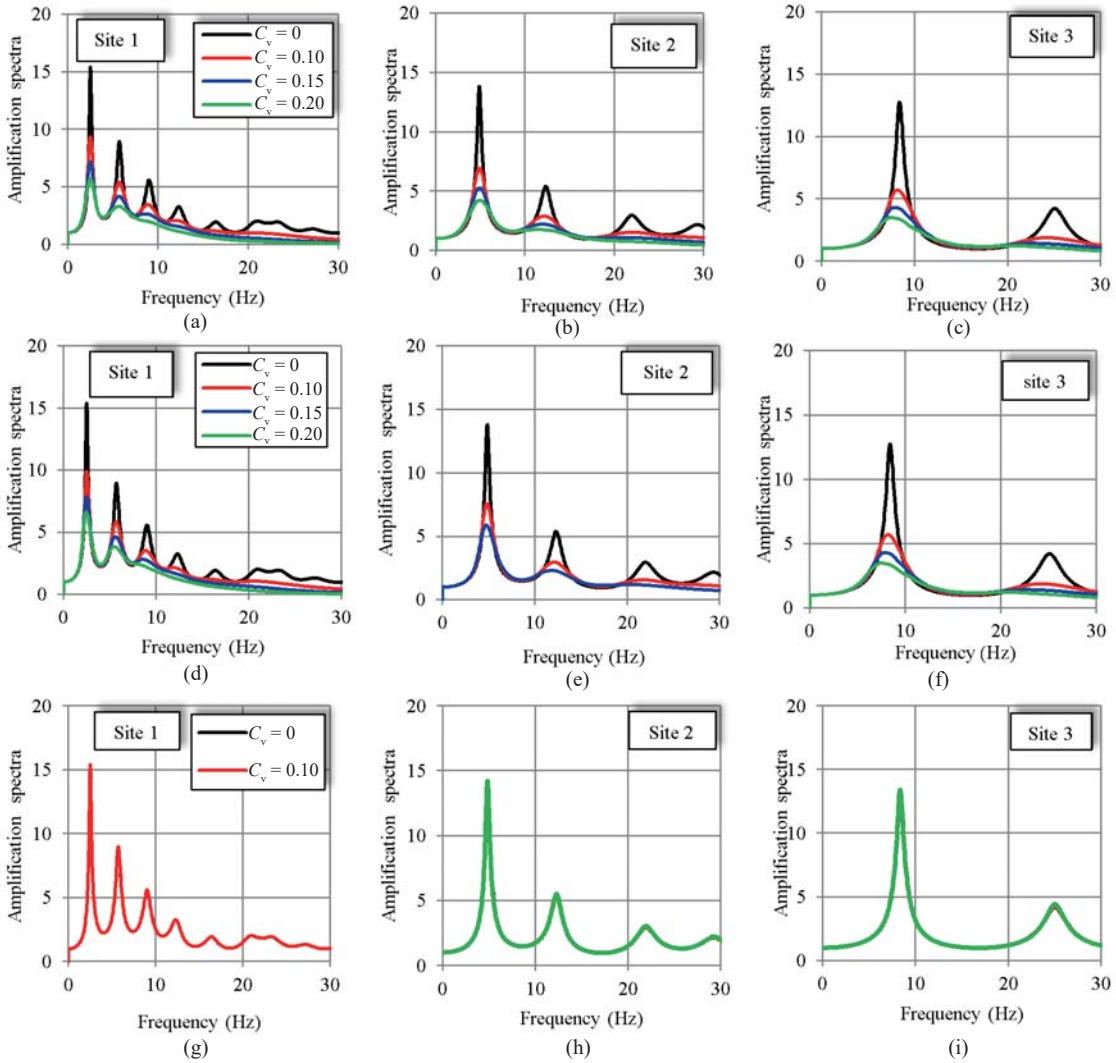

Fig. 3 Mean amplification function for different soil conditions: (a), (b), (c) effect of random wave velocity, (d), (e), (f) effect of random thickness, (g), (h), (i) effect of random damping ratio

Thus, since the randomness of the damping ratio does not influence the amplification function, only the random variations of correlated velocity and thickness are deeply examined. First, Figure 4 depicts the mean amplification functions due to the randomness and correlation (ρ_{Vsd}) between the wave velocity V_s and the thickness (h). No significant differences appear between the curves of Figs. 4(a), 4(b), 4(c) and Figs. 4(d), 4(e), 4(f) due to the low correlation between the two parameters; however, for higher coefficients of correlation, the amplification function amplitudes are more influenced by the random variations of the soil parameters (Figs. 4(g)-4(l)). In particular, for completely correlated parameters (ρ_{Vsh} = 1), variability effects of the soil conditions are more apparent (Figs. 4(j)-4(k)). In fact, for soil profile number 1, when the wave velocity

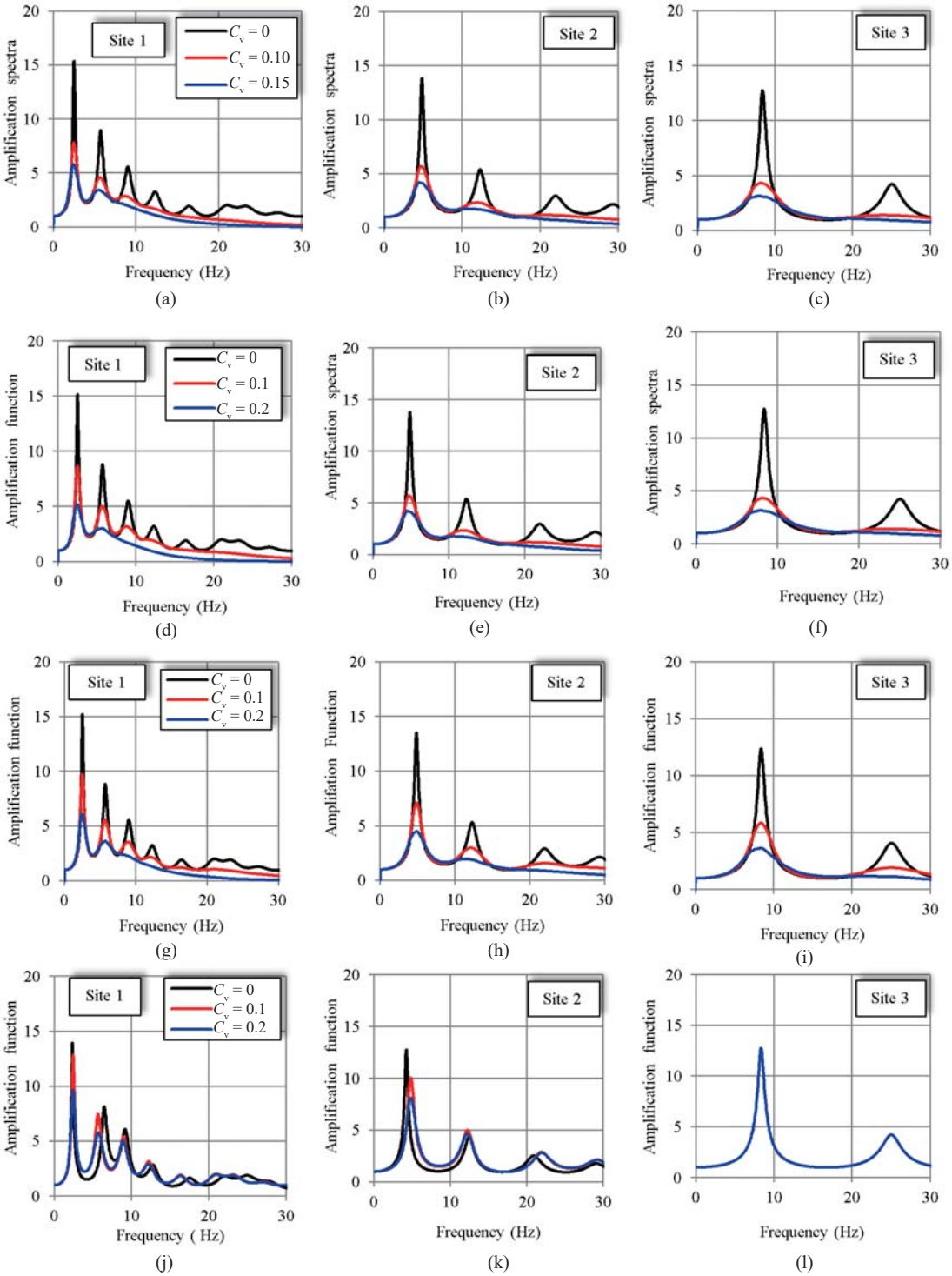

Fig. 4 Mean amplification function for Gaussian velocity and thickness: (a), (b), (c) uncorrelated, (d), (e), (f) correlated with ρ_{Vsh} = 0.3, (g), (h), (i) correlated with ρ_{Vsh} = 0.6, (j), (k), (l) correlated with ρ_{Vsh} = 1

and thickness are assumed to be completely correlated, the amplification function amplitudes show less of a decrease than in the uncorrelated case (Figs. 3(a)-3(f)) and the higher natural frequencies are shifted to the left, meaning that the soil becomes softer as the randomness of the medium increases. The same observations may be made for soil profile number 2 but due to the shift of the natural frequencies to the right, the soil deposit becomes harder. Soil deposit number 3 remains insensitive to random velocity and thickness. These different behaviors of the three different soil deposits explain the effects of the random and spatial variations of the soil conditions on the amplification of ground motions and encourage the need to take them into consideration in any site response analysis.

5.2 Stochastic surface ground motions

In the following application, under the assumption of correlated random velocity and thickness, stochastic spatial PSD is computed and the stochastic spatially varying ground acceleration and response spectra at the three different ground surface locations (Fig. 1) are computed. The incident base rock motions are assumed to have the same intensities and are displayed by the filtered Clough and Penzien (1993) PSD function. In a simplified way, the auto- and cross-PSD functions are calculated (Eq. (3)) based on the mean amplification functions according to the algorithm in Fig. 2. Figure 5 shows the auto-PSD functions for the three soil conditions at the studied sites. It is clear that the mean auto-PSD magnitudes change in similar way as the mean amplification function magnitudes.

2048 frequency samples are used to obtain the mean cross-PSD and to generate the spatially varying frequency-histories using the above scheme. The duration is $T = 20$ s and the parameters of the Clough and Penzien (1993) filter are assumed as $\omega_f = 0.5\pi$, $\omega_g = 6\pi$, $\xi_g = \xi_f = 0.6$ and $S_0 = 0.0565$ m^2/s^3. Two examples are carried out to distinguish the influence of the coherency model in simulating spatially varying ground motion. The separation distances between points 1 & 2 and 1 & 3 in Fig. 1 are 100 m and 200 m, respectively.

Example 1

In order to study the incoherency between base rock accelerations at locations j' and k' (j', $k' = 1, 3$), the Sobczyk (1991) model (Eqs. (11)) is selected in the first example:

$$\gamma_{j'k'}(\mathrm{i}\omega) = \left|\gamma_{j'k'}(\mathrm{i}\omega)\right| \exp\left(-\mathrm{i}d_{j'k'}\cos/V_{\mathrm{app}}\right)$$

or

$$\gamma_{j'k'}(\mathrm{i}\omega) = \exp\left(-d_{j'k'}^2/V_{\mathrm{app}}\right)\exp\left(-\mathrm{i}d_{j'k'}\cos/V_{\mathrm{app}}\right) \quad (11)$$

in which b is a parameter controlling the incoherency and is taken as equal to 0.002 (Bi and Hao, 2012). The incident angle of *SH* wave a is assumed to be 0° here. The apparent wave velocity V_{app} is taken as equal to 2500 m/s.

As shown in Fig. 6, the coherency values for the Sobczyk (1991) model decrease rapidly versus frequency as the separation distance between sites increases due to the exponential variation (Eq. (11)).

Stochastically simulated base rock and ground surface acceleration time-histories are depicted in Figs. 7 and 8, respectively, for the same C_v of the velocity (V_{sl}) and thickness (h_l) as in the preceding example (0%, 10% and 20%). The peak ground accelerations (PGAs) at the ground surface positions of 1, 2 and 3 are, respectively, 5.98, 7.55 and 7.13 m/s² in the determinist case ($C_v = 0.0$), which are much greater than base rock PGAs (1.80, 2.29 and 6.06 m/s²) for locations 1′, 2′ and 3′ because of the amplification due to the variation of the soil conditions in the vertical direction. As the coefficients of variation

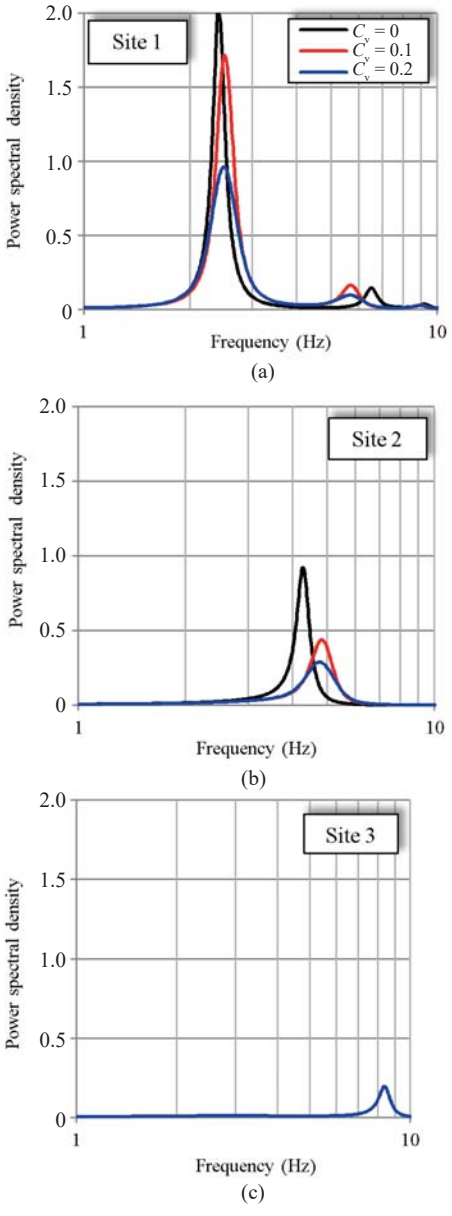

Fig. 5 Mean spectral densities on ground surface

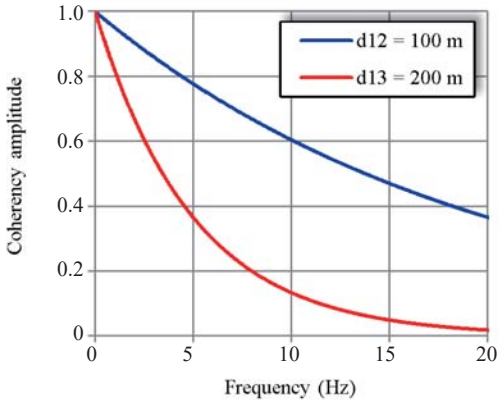

Fig. 6 Site coherency via the Sobczyk (1991) model

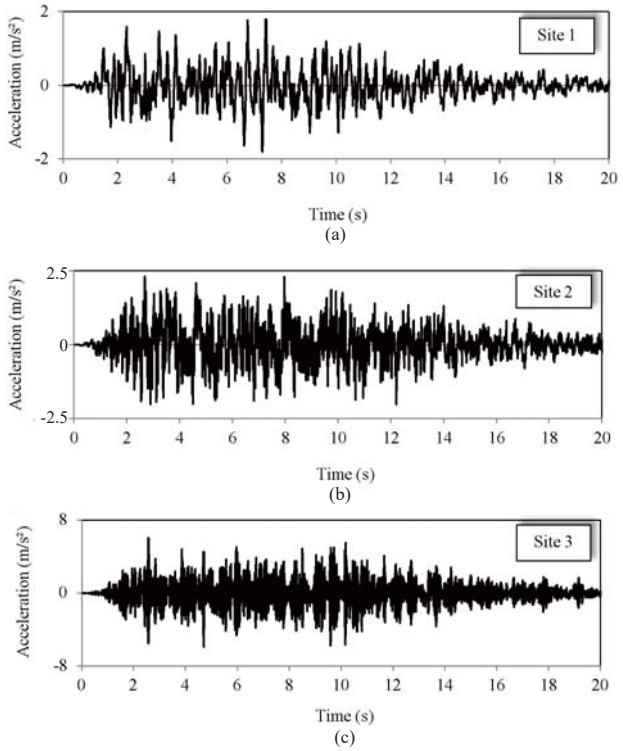

Fig. 7 Simulated bedrock acceleration time-histories using the Sobczyk (1991) model coherency

increase (10% and 20%) for the three sites, the ground surface PGAs decrease in accordance with the influence of fluctuations around the velocity and thickness on the amplitudes of the amplification function and PSD function. This result is similar to that obtained by Sadouki *et al*. (2012) that considered the shear modulus as a random parameter and concluded that this trend is due to medium randomness, which created multiples reflections and refractions of the incident wave. Thus, it may be concluded that simulated ground motions at the surface of media with random parameters with the aid of Monte Carlo methods present similar trends as those obtained by rigorous analytical methods.

Stochastic spatially varying response spectra are obtained at the three ground locations (1, 2, 3) (Fig. 1) as shown in Fig. 9 for coefficients of variation (C_v) of the wave velocity and thickness equal to 0, 10% and 20%. This figure shows that the spectral ordinates decrease as the C_v increases, meaning that as the random heterogeneity of the medium becomes more important, the spectral ordinates attenuate (Figs. 9(a)-9(b)) but the spectral shape is preserved for a same site. Response spectra at site 3 remains insensitive to the randomness of the soil properties (Fig. 9(c)).

Therefore, the randomness of the soil properties significantly affects ground surface response spectra. The site most affected by this randomness is the first one because it is deeper than the other two sites and consequently the soil parameters' randomness has more influence. This conservative result could affect the seismic response of multi-support and/or underground structures, which may be excited by such response spectra during their seismic resistant analysis and design.

Example 2

The Sobczyk (1991) coherency model is appropriate for short separation distances. For longer separation distances and higher frequencies, the model of Harichandran and Vanmarcke (1986) is more appropriate to represent the incoherency. However, for comparative purposes, the short separation distances in the first example are maintained. The Harichandran and Vanmarcke (1986) model takes the form:

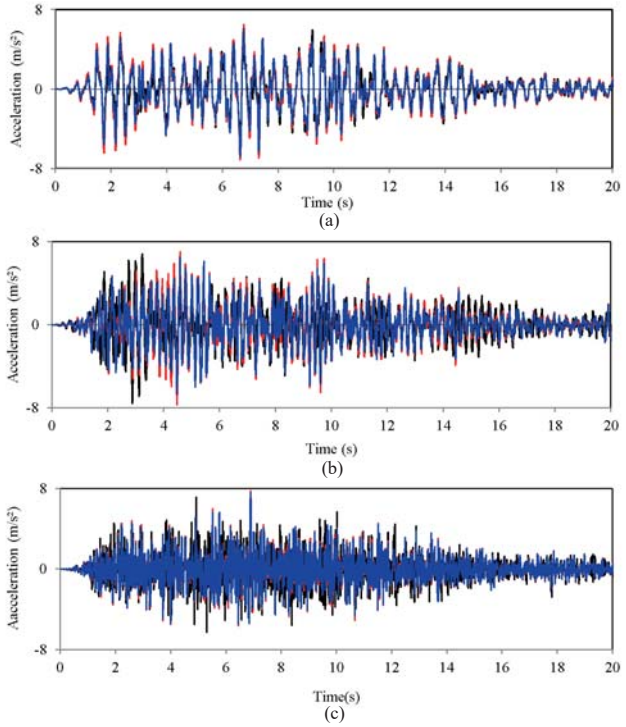

Fig. 8 Simulated ground surface acceleration time-histories using the Sobczyk (1991) coherency model with correlated Gaussian velocity and thickness (ρ_{Vsh} = 1)

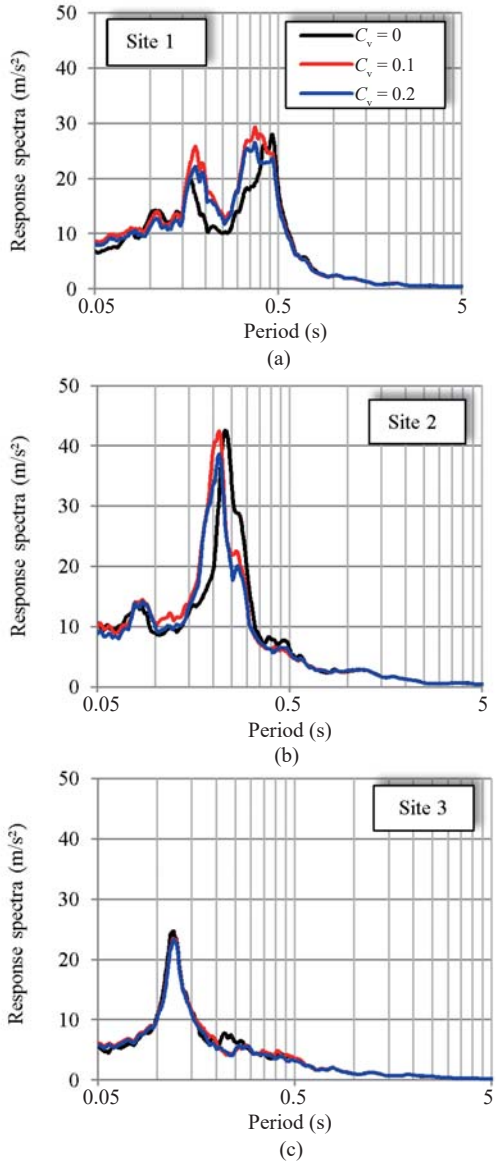

Fig. 9 Stochastic spatially varying response spectra using Sobczyk (1991) coherency model

$$\left|\gamma_{j'k'}(\mathrm{i}\omega)\right| = A\exp\left(-\frac{2d_{j'k'}}{\alpha\theta(f)}(1-A+\alpha A)\right) + (1-A)\exp\left(-\frac{2d_{j'k'}}{\theta(f)}(1-A+\alpha A)\right) \quad (12)$$

where

$$\theta(f) = k\left(1+\left(f/f_0\right)^{\mathrm{B}}\right)^{-1/2} \quad (13)$$

such that f is the frequency (Hz). The model parameters values (A = 0.636, B = 2.95A, α = 0.0186, f_0 = 1.51 Hz and k = 31200) are defined based on an analysis of the SMART-1 array records. The Harichandran and Vanmarcke (1986) site coherency is plotted in Fig. 10 where similar values are obtained at low frequencies (less than 5 Hz) compared to the Sobczyk (1991) model, where the coherency approaches to zero faster (Eq. (11) and Fig. 6) while the coherency in Fig. 10 decays slowly with frequency (Eq. (12)).

The simulated base rock accelerations time-histories are depicted in Fig. 11. PGAs obtained by this model are 1.48, 1.36 and 1.62 m/s² at the locations 1′, 2′ and 3′, respectively. They are smaller than those obtained by the first model. Note that this model evaluates the coherency directly from the data recorded so that the variability due to the lagged coherency estimates could be clearly observed.

Figure 12 shows the simulated ground surface

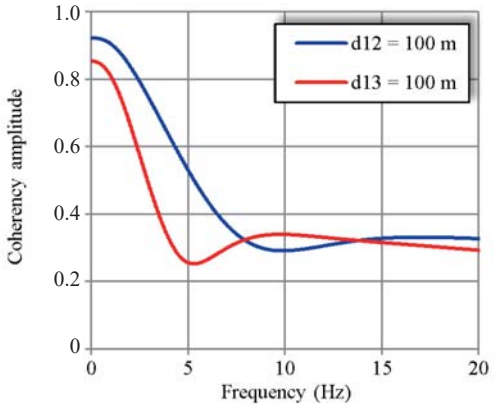

Fig. 10 Site coherency via the Harichandran and Vanmarcke (1986) model

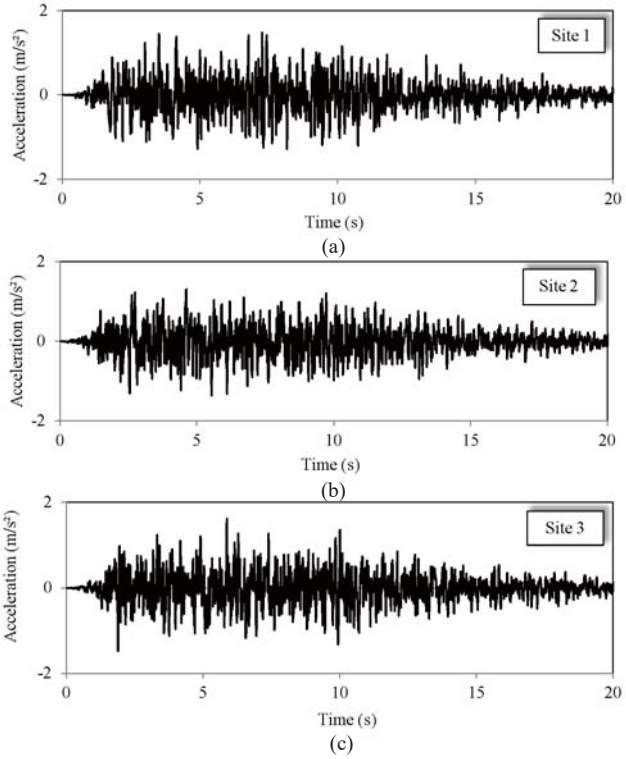

Fig. 11 Simulated bedrock acceleration time-histories using the Harichandran and Vanmarcke (1986) coherency model

accelerations. The PGAs at locations 1, 2 and 3 are, respectively, 7.70, 4.57, 4.66 m/s² (in the determinist case) which are different from those obtained by the first coherency model (5.98, 7.55, 7.13 m/s²), but as in the previous example the ground surface PGAs decrease when the coefficients of variation increase (10% and 20%) for the different sites.

The response spectra obtained using the Harichandran and Vanmarcke (1986) model are plotted in Fig. 13. The stochastic response spectra obtained by the Sobczyk (1991) model (Fig. 9) and those obtained by the Harichandran and Vanmarcke (1986) model (Fig. 13) show a similar trend but the spectral ordinates could not be compared because coefficients defining the two models are obtained differently.

6 Conclusions

This study investigated the effects of the randomness of soil layers on the ground surface accelerations and response spectra using Monte Carlo methods. These effects on the amplification of the surface ground motions are studied considering the soil parameters that influence the ground response (thicknesses, velocities and damping of the layers) as Gaussian (or normal) random variables generated many times via Monte Carlo methods. In order to obtain spatially varying seismic ground surface motions at multiple locations due to surface irregularities, a reasonable procedure based on the one dimensional *SH* wave propagation together with the definition of cross spectral densities was followed. The incident motion is assumed as having the same spectral density at the base rock and the effects of the loss of coherence were described using the Sobczyk (1991) and the Harichandran and Vanmarcke (1986) models. Stochastic and site dependent spatially varying ground surface motions were predicted by means of the spectral representation method and the corresponding surface response spectra were obtained by solving the equation of motion of a linear SDOF system under a

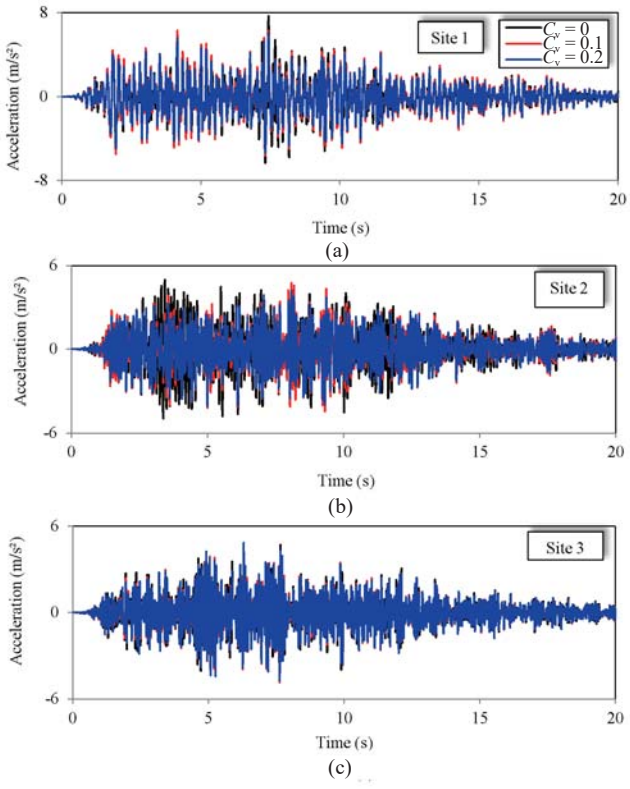

Fig. 12 Simulated ground surface acceleration time-histories using the Harichandran and Vanmarcke (1986) coherency model with correlated Gaussian velocity and thickness (ρ_{Vsh} = 1)

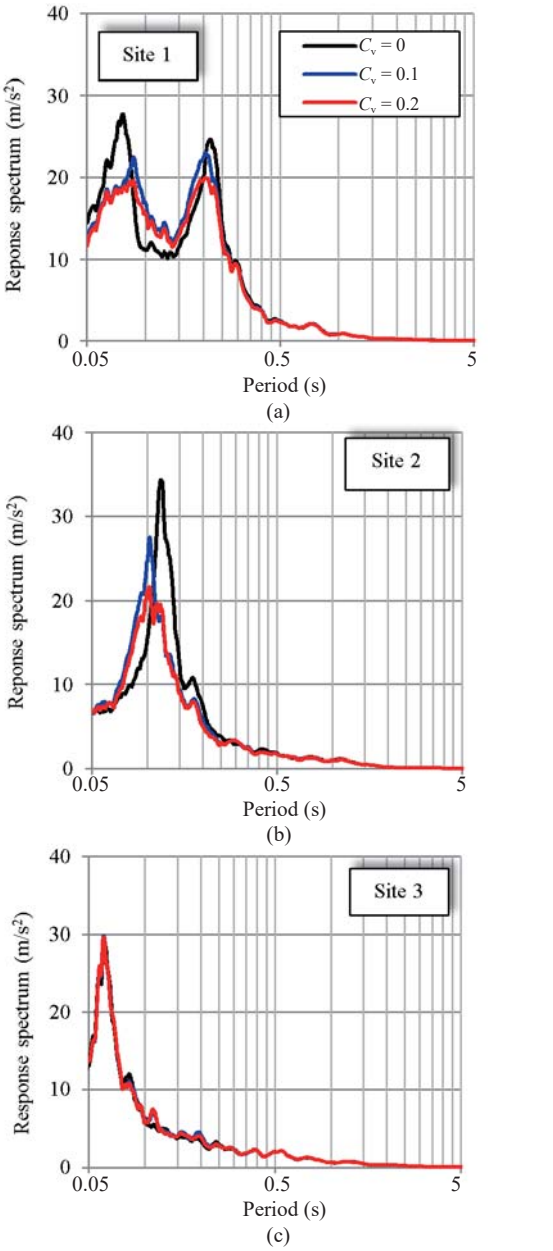

Fig. 13 Stochastic spatially varying response spectra using the Harichandran and Vanmarcke (1986) coherency model

nonstationary stochastic process.

The results indicate that the random variations of the soil properties (velocities and thicknesses of layers in the present study) affect the magnitudes of the amplification function and the PSD and consequently the simulated ground movements.

Clearly, response spectra are very sensitive to the inherent spatial variation of soil properties and soil conditions variation in vertical as well as horizontal directions. Also, both the Sobczyk (1991) model and Harichandran and Vanmarcke (1986) model successfully help simulate ground motions for short separation distances. The simulated response spectra may serve as inputs in the seismic resistant analysis and design of multi-supported and underground structures. The variations in response spectra due to the randomness of the soil layers may significantly alter the response of multi-supported structures that were eventually excited by such data than by uniform ground motions.

References

Adanur S, Altunişik AC and Soyluk K, Bayraktar A, Dumanoğlu A (2016), "Multiple-Support Seismic Response of Bosporus Suspension Bridge for Various Random Vibration Methods," *Case Studies in Structural Engineering*, **5**: 54–67.

Alam MI and Kim D (2014), "Spatially Varying Ground Motion Effects on Seismic Response of Adjacent Structures Considering Soil-Structure Interaction," *Advances in Structural Engineering*, **17**(1): 131–142.

Badaoui M, Berrah MK and Mebarki A (2010), "Stochastic Seismic Response of Multi-Layered Soil with Random Layer Heights," *Earthquake Engineering and Engineering Vibration*, **9**(2): 213–221.

Bi K and Hao H (2011), "Influence of Irregular Topography and Random Soil Properties on Coherency Loss of Spatial Seismic Ground Motions," *Earthquake Engineering & Structural Dynamics*, **40**(9): 1045–1061.

Bi K and Hao H (2012), "Modelling and Simulation of Spatially Varying Earthquake Ground Motions at Sites with Varying Conditions," *Probabilistic Engineering Mechanics*, **29**: 92–104.

Cacciola P and Deodatis G (2011), "A Method for Generating Fully Non-Stationary and Spectrum-Compatible Ground Motion Vector Processes," *Soil Dynamics and Earthquake Engineering*, **31**: 351–360.

Cacciola P and D'Amico L (2015), "Response Spectrum Compatible Ground Motion Processes," In: Beer M, Kougioumtzoglou IA, Patelli E, Au I, eds. *Encyclopedia of Earthquake Engineering*, Springer, Berlin Heidelberg, 1–27, ISBN 97836423619750.

Cho SE (2007), "Effects of Spatial Variability of Soil Properties on Slope Stability," *Engineering Geology*, **92**: 97–109.

Chouw N and Hao H (2005), "Study of SSI and Non-Uniform Ground Motion Effect on Pounding Between Bridge Girders," *Soil Dynamics and Earthquake Engineering*, **25**(7–10): 717–728.

Chouw N and Hao H (2008), "Significance of SSI and Nonuniform Near-Fault Ground Motions in Bridge Response I: Effect on Response with Conventional Expansion Joint," *Engineering Structures*, **30**(1): 141–153.

Clough RW and Penzien J (1993), *Dynamics of structures*, New York: McGraw Hill.

Davoodi M, Jafari MK and Sadrolddini SMA (2013), "Effect of Multi-Support Excitation on Seismic Response of Embankment Dams," *International Journal of Civil Engineering, B: Geotechnical Engineering*, **11**(1): 19–28.

Der Kiureghian A (1996), "A Coherency Model for Spatially Varying Ground Motions," *Earthquake Engineering and Structural Dynamics*, **25**(1): 99–111.

Deodatis G (1996), "Nonstationary Stochastic Vector Processes: Seismic Ground Motion Applications," *Probabilistic Engineering Mechanics*, **11**(3): 149–167.

Djilali Berkane H, Khellafi A, Harichane Z and Kouci W (2014), "Stochastic Study of the Spatial Variation of Ground Response Spectrum," *Electronic Journal of Geotechnical Engineering*, **13**(B): 1–17.

Djilali Berkane H, Harichane Z, Guellil ME Sadouki A (2019), "Investigation of Soil Layers Stochasticity Effects on the Spatially Varying Seismic Response Spectra," *Indian Geotechnical Journal*, **49**(2): 151–160.

Elkateb T, Chalaturnyk R and Robertson PK (2002), "An Overview of Soil Heterogeneity: Quantification and Implications on Geotechnical Field Problems," *Canadian Geotechnical Journal*, **40**: 1–15.

Gao Q, Lin JH, Zhong WX, Howson WP and Williams FW (2008), "Propagation of Partially Coherent Non-Stationary Random Waves in a Viscoelastic Layered Half-Space," *Soil Dynamics and Earthquake Engineering*, **28**(4): 305–320.

Giaralis A and Spanos PD (2012), "Derivation of Response Spectrum Compatible Non-Stationary Stochastic Processes Relying on Monte Carlo-Based Peak Factor Estimation," *Earthquakes and Structures*, **3**(3-4): 581–609.

Guellil ME, Harichane Z, Djilali Berkane H and Sadouki A (2017), "Soil and Structure Uncertainty Effects on the Soil Foundation Structure Dynamic Response," *Earthquakes and Structures*, **12**(2): 153–163.

Haciefendioglu K (2010), "Effect of Material Uncertainty on Stochastic Response of Dams," *Proceedings of the Institution of Civil Engineers Geotechnical Engineering*, **163**(2): 83–89.

Harichandran RS and Vanmarcke EH (1986), "Stochastic Variation of Earthquake Ground Motion in Space and

Time," *Journal of Engineering Mechanics*, **112**(2): 154–174.

Harichane Z, Afra H and Elachachi SM (2005), "An Identification Procedure of Soil Profile Characteristics from Two Free Field Accelerometer Records," *Soil Dynamics and Earthquake Engineering*, **5**(8): 431–438.

Hao H, Oliveira CS and Penzien J (1989), "Multiple-Station Ground Motion Processing and Simulation Based on SMART-1 Array Data," *Nuclear Engineering and Design*, **111**(3): 193–310.

Hao H (1998), "Parametric Study of the Required Seating Length for Bridge Decks during Earthquake," *Earthquake Engineering and Structural Dynamics*, **27**(12): 91–103.

He J (2015) "Karhumen-Loéve Expansion for Random Earthquake Excitations," *Earthquake Engineering and Engineering Vibration*, **14**(1): 77–84.

Konakli K and Der Kiureghian A (2011), "Stochastic Dynamic Analysis of Bridges Subjected to Spatially Varying Ground Motions," *PEER Report 2011/105*.

Li C, Li H, Hao H, Bi K and Tian L (2018), "Simulation of Multi-Support Depth-Varying Earthquake Ground Motions Within Heterogeneous Onshore and Offshore Sites," *Earthquake Engineering and Engineering Vibration*, **17**(3): 475–490.

Li W and Assimaki D (2010), "Site- and Motion-Dependent Parametric Uncertainty of Site-Response Analyses in Earthquake Simulations," *Bulletin of the Seismological Society of America*, **100**(3): 954–968.

Lin JH, Zhang YH and Zhao Y (2004), "Seismic Spatial Effects on Dynamic Response of Long-Span Bridges in Stationary Inhomogeneous Random Fields," *Earthquake Engineering and Engineering Vibration*, **3**(2): 171–180.

Loh CH and Lin SG (1990), "Directionality and Simulation in Spatial Variation of Seismic Waves," *Engineering Structures*, **12**(2): 134–143.

Lou L and Zerva A (2005), "Effects of Spatially Variable Ground Motions on the Seismic Response of a Skewed," Multi-Span, RC Highway Bridge," *Soil Dynamics and Earthquake Engineering*, **25**(7–10): 729–740.

Mwafy AM, Kwon OS, Elnashai A and Hashash YMA (2011), "Wave Passage and Ground Motion Incoherency Effects on Seismic Response of an Extended Bridge," *Journal of Bridge Engineering*, **16**(3): 364–374.

Nigam NC and Jennings PC (1969), "Digital Calculation of Response Spectra from Strong-Motion Earthquake Records," *Bulletin of the Seismological Society of America*, **59**(2): 909–922.

Phoon KK and Kulhawy FH (1999), "Characterization of Geotechnical Variability," *Canadian Geotechnical Journal*, **36**(4): 612–624.

Popescu R, Deodatis G and Nobahar A (2005), "Effects of Random Heterogeneity of Soil Properties on Bearing Capacity," *Probabilistic Engineering Mechanics*, **20**: 324–341.

Popescu R (2008), "Effects of Soil Spatial Variability on Liquefaction Resistance: Experimental and Theoretical Investigations," *Proceeding of the 4th International Symposium on Deformation Characteristics of Geomaterials* (IS-Atlanta).

Sadouki A, Harichane Z and Chehat A (2012), "Response of a Randomly Inhomogeneous Layered Media to Harmonic Excitations," *Soil Dynamics and Earthquake Engineering*, **36**: 84–95.

Sadouki A, Harichane Z, Elachachi SM and Erken A (2018), "Response of Anisotropic Porous Layered Media with Uncertain Soil Parameters to Shear Body- and Love-Waves," *Earthquakes and Structures*, **14**(4): 313–322.

Saxena V, Deodatis G and Shinozuka M (2000), "Effect of Spatial Variation of Earthquake Ground Motion on the Nonlinear Dynamic Response of Highway Bridges," *Proc of 12th World Conf on Earthquake Engineering*, Auckland, New Zealand.

Shrikhande M and Gupta VK (1998), "Synthesizing Ensembles of Spatially Correlated Accelerograms," *Journal of Engineering Mechanics*, **124**(11): 1185–1192.

Sobczky K (1991), *Stochastic Wave Propagation*, Netherlands: Kluwer Academic Publishers.

Wolf JP (1985), *Dynamic Soil–Structure Interaction*, Englewood Cliffs (NJ): Prentice Hall.

Yang Q, Saiid MS, Hang W and Itani A (2002), "Influence of Earthquake Ground Motion Incoherency on Multi-Support Structures," *Earthquake Engineering and Engineering Vibration*, **1**(2): 167–180.

Yazdani A and Takada T (2011)," Probabilistic Study of the Influence of Ground Motion Variables on Response Spectra," *Structural Engineering and Mechanics*, **39**(6): 877–893.

Ye JH, Zhang ZQ and Liu XM (2012), "A Simplified Multisupport Response Spectrum Method," *Earthquake Engineering and Engineering Vibration*, **11**(2): 243–256.

Zerva A (1992), "Spatial Incoherence Effects on Seismic Ground Strains," *Probabilistic Engineering Mechanics*, **7**: 217–226.

Zerva A and Zervas V (2002), "Spatial Variation of Seismic Ground Motions: an Overview," *Applied Mechanics Reviews*, **56**(3): 271–297.

Zhang DY, Jia HY, Zheng SX, Xie WC and Pandey MD (2014), "A Highly Efficient and Accurate Stochastic Seismic Analysis Approach for Structures under Tridirectionally Nonstationary Multiple Excitations," *Computers and Structures*, **145**: 23–35.

Zhang DY, Liu W, Xie WC and Pandey MD (2013), "Modeling of Spatially Correlated Site-Reflected and Non-Stationary Ground Motions Compatible with Response Spectrum," *Soil Dynamics and Earthquake Engineering*, **55**: 21–32.

Appendix

Solution of wave equation

The solution of Eq. (9), for a harmonic motion in each layer l (l = 1, N_C, Fig. 1) is:

$$u_l(z_l,t) = U_l(z_l)\,\mathrm{e}^{\mathrm{i}\omega t} \tag{A1}$$

considering a coordinate system z_l for each layer in a vertically downward direction with the origin at the top of the layer $0 \le z_l \le h_l$ where h_l is the thickness of the lth layer) and $U_l(z_l)$ is the depth-dependent displacement taking the equation:

$$u_l(z_l,t) = A_l\mathrm{e}^{\mathrm{i}P_l z_l} + A'_l\,\mathrm{e}^{-\mathrm{i}P_l z_l} \tag{A2}$$

with $p_l = \dfrac{\omega \cdot \cos\alpha_l}{V_{sl}}$. The incident and reflected wave amplitudes (A_l and A'_l) in each layer l are obtained from the boundary conditions (Harichane *et al.*, 2005) leading to:

$$A_{l+1} = \frac{1}{2}A_l(1+q_l)\cdot\mathrm{e}^{\mathrm{i}.p_l.h_l} + \frac{1}{2}A_l^{'}(1-q_l)\cdot\mathrm{e}^{-\mathrm{i}.p_l.h_l} \tag{A3}$$

$$A_{l+1}^{'} = \frac{1}{2}A_l(1-q_l)\cdot\mathrm{e}^{\mathrm{i}.p_l.h_l} + \frac{1}{2}A_l^{'}(1+q_l)\cdot\mathrm{e}^{-\mathrm{i}.p_l.h_l} \tag{A4}$$

where $q_l = \sqrt{(\rho_l.G_l / \rho_{l+1}.G_{l+1})}.(\cos\alpha_l / \cos\alpha_{l+1})$

G_l and ρ_l are the shear modulus and mass density of the lth layer of a soil deposit (Fig. 1) related by $G_l = V_{sl}^2\rho_l$.

The hysteretic damping ξ_l may be introduced by the complex velocity of the *SH* wave in the form ($V_{sl}^* = V_{sl}\sqrt{1+2\mathrm{i}\xi_l}$). Therefore, all the above equations hold by replacing V_{sl} by V_{sl}^*.

Response spectrum evaluation

Numerical integration, according to the Nigam and Jenning (1969) technique, of the governing equation of a SDOF system:

$$\ddot{x}(t) + 2\zeta\omega_\mathrm{n}\dot{x}(t) + \omega_\mathrm{n}^2 x(t) = -\ddot{u}_\mathrm{g}(t) \tag{A5}$$

where ζ is the critical viscous damping, ω_n is the natural frequency, and $\ddot{u}_\mathrm{g}(t)$ is the ground motion (Eq. (7)), allows the relative displacement response spectrum $S_d(\omega_\mathrm{n}, \zeta)$, to be obtained formally as

$$S_d(\omega_\mathrm{n},\zeta) = \max\left\{\left|x(t)\right|\right\} \tag{A6}$$

And the pseudo response spectrum is:

$$S_a(\omega_\mathrm{n},\zeta) = \omega^2 S_d(\omega_\mathrm{n},\zeta) \tag{A7}$$